

# $T_0$ censorship of early dark energy and AdS vacua

Gen Ye<sup>1\*</sup> and Yun-Song Piao<sup>1,2,3,4†</sup>

<sup>1</sup> *School of Physics, University of Chinese Academy of Sciences, Beijing 100049, China*

<sup>2</sup> *Institute of Theoretical Physics, Chinese Academy of Sciences,  
P.O. Box 2735, Beijing 100190, China*

<sup>3</sup> *School of Fundamental Physics and Mathematical Sciences,  
Hangzhou Institute for Advanced Study,  
UCAS, Hangzhou 310024, China and*

<sup>4</sup> *International Center for Theoretical Physics Asia-Pacific, Beijing/Hangzhou, China*

## Abstract

Present-day temperature  $T_0$  of cosmic microwave background has been precisely measured by the FIRAS experiment. We identify that the early dark energy (EDE) (non-negligible around matter-radiation equality) scenario can remain compatible with the FIRAS result, while lifting the Hubble constant  $H_0$ . We perform Monte Carlo Markov chain analysis to confirm our observations. We also present an  $\alpha$ -attractor Anti-de Sitter (AdS) model of EDE, in which the AdS depth is consistently varied in the Monte Carlo Markov chain analysis. We found that our datasets weakly hinted the existence of an AdS phase near recombination with  $H_0 \sim 73\text{km/s/Mpc}$  at  $1\sigma$  region in the best-fit model.

PACS numbers:

---

\* yegen14@mailsucas.ac.cn

† yspiao@ucas.ac.cn

## I. INTRODUCTION

The Hubble constant  $H_0$ , the present-day expansion rate of the Universe, sets the scale of the current Universe. Local measurements of  $H_0$  yield  $H_0 \gtrsim 73\text{km/s/Mpc}$  [1–4] (e.g.the SH0ES group reports  $H_0 = 74.03 \pm 1.42\text{km/s/Mpc}$  [4, 5]), which shows  $> 4\sigma$  discrepancy [6] compared with the Planck result  $H_0 = 67.72 \pm 0.40\text{km/s/Mpc}$  [7]. This discrepancy (called “*Hubble tension*”) can hardly be explained by systematic errors [8].

However, the analysis of Planck is based on  $\Lambda\text{CDM}$  and probes of high redshift physics, i.e. cosmic microwave background (CMB) and baryon acoustic oscillations (BAO). Thus the Hubble tension might be a hint of beyond- $\Lambda\text{CDM}$  physics, specially before recombination [9–12]. One possibility is early dark energy (EDE) [13–22] (see also [23–25] for modified gravity). EDE is non-negligible only for a short period near matter-radiation equality and before recombination (the Universe after recombination is  $\Lambda\text{CDM}$ -like), which results in a suppressed sound horizon, and thus  $H_0 \gtrsim 70\text{km/s/Mpc}$ .

Recently, it has been found in Ref.[20] that the existence of Anti de-Sitter (AdS) vacua around recombination can effectively lift  $H_0$  to  $\sim 73\text{km/s/Mpc}$  at  $1\sigma$  region. The cosmologies with an AdS phase at low- $z$  have been studied in Refs.[26–28]. The AdS vacua is ubiquitous in the landscape (consisting of all effective field theories with consistent UV-completion) [29, 30], see also [31, 32] for inflation with multiple AdS vacua. The AdS potential in Ref.[20] is only a phenomenological one with the AdS depth being fixed by hand rather than varied in the analysis. Thus it is significant to search for AdS-EDE models originating from UV-complete theories in the cosmological setup with varying AdS depth in the Monte Carlo Markov Chain (MCMC) analysis .

Precise measurement of the present-day CMB  $T_0$  from the COBE/FIRAS experiment, independent of Planck, yields [33, 34]

$$T_{0,FIRAS} = 2.72548 \pm 0.00057K. \tag{1}$$

Based on  $\Lambda\text{CDM}$ , the Planck and BAO data yields  $T_0 = 2.718 \pm 0.021K$  [35], consistent with  $T_{0,FIRAS}$ . However, the  $T_0$  deduced from the Planck and SH0ES data, assuming  $\Lambda\text{CDM}$ , has  $> 4\sigma$  discrepancy compared with  $T_{0,FIRAS}$ , called  $T_0$  tension in Ref.[36], see also [37, 38] for recent studies. This might be yet another hint of new physics beyond  $\Lambda\text{CDM}$ .

In this paper, we identify, at the cosmological parameter level, how the EDE scenario lifts  $H_0$ , while staying compatible with  $T_{0,FIRAS}$ , at the cost of a parameter shift to a larger  $\omega_m$ .

We perform MCMC analysis to confirm our observations. We also present a theoretically well-motivated AdS-EDE model as well as the corresponding MCMC analysis with the AdS depth consistently varied. It is noticed that the full datasets weakly hinted the existence of an AdS phase near recombination. Low- $z$  resolutions to the Hubble tension have also been discussed, see e.g.[39–42] for different perspectives. As a contrast, we also show that  $w$ CDM models with a constant equation of state parameter  $w \lesssim -1.3$  of dark energy at low- $z$  seem incompatible with  $T_{0,FIRAS}$ . Throughout this paper we assume a spatially flat Universe.

## II. EARLY DARK ENERGY AND ADS

EDE may be non-negligible only for a short epoch decades before recombination [13, 14]. The injection of EDE energy results in a larger Hubble rate  $H(z \gtrsim z_{rec})$  prior to recombination, so a suppressed sound horizon  $r_s = \int_{z_{rec}}^{\infty} dz/H(z)$ . The spacing of CMB acoustic peaks perfectly sets the angular scale  $\theta_{CMB}$ ,

$$\theta_{CMB} = \frac{r_s(z_{rec})}{D_A(z_{rec})}, \quad (2)$$

where

$$D_A(z_{rec}) \equiv \int_0^{z_{rec}} \frac{dz}{H(z)} = \frac{1}{T_0} \int_{T_0}^{T_{rec}} \frac{dT}{H(T)} \quad (3)$$

and  $z_{rec} \sim 1100$  is the recombination redshift.  $D_A(z_{rec})$  is the comoving angular distance, which is sensitive only to post recombination physics. Generally,  $D_A$  is anti-correlated with  $H_0$ , so for constant  $\theta_{CMB}$ ,  $H_0 \sim r_s^{-1}$  will increase.

In the AdS-EDE model [20], initially the scalar field sits at the hillside of its potential  $V(\phi)$ , and  $\rho_\phi$  is negligible. It will roll down the potential sometime near matter-radiation equality (when  $\rho_\phi/\rho_{tot} \sim 10\%$ ), and roll into an AdS phase. In the AdS region, we have  $w_\phi = p_\phi/\rho_\phi > 1$ , so that  $\rho_\phi \sim a^{-3(1+w)}$  will more quickly redshift away (in Refs.[13, 14, 17] the dissipation of  $\rho_\phi$  is less effective by oscillation with cycle-averaged  $w < 1$ , see also Refs.[18, 22] for different mechanisms). This is crucial for having a larger injection of  $\rho_\phi$  ( $> 10\%$ ), thus a higher  $H_0$ .  $\rho_\phi$  injected must be dissipated rapidly enough so that it is negligible around recombination, or it will interfere with the fit of  $\Lambda$ CDM to CMB data. After that, the field will climb up to the  $\Lambda > 0$  region, and the Universe is settled to be  $\Lambda$ CDM-like until now.

The potential  $V(\phi)$  in Ref.[20] is only a phenomenological one constructed by gluing a  $\phi^4$  like AdS minima with a late cosmological constant phase. Inspired by the  $\alpha$ -attractor [43, 44], we take  $V(\phi)$  as (see Fig-1)

$$V(\phi) = V_0 \left[ 1 - \exp \left( -\gamma \tanh \left( \frac{\phi}{M_p \sqrt{6\alpha}} \right) \right) \right]^2 - V_0 + V_\Lambda. \quad (4)$$

For  $\phi \ll -M_p(6\alpha)^{1/2}$ , we have a high plateau  $V(\phi) \sim e^{2\gamma}V_0$  responsible for EDE. For  $\phi \gg M_p(6\alpha)^{1/2}$ ,  $V(\phi) = V_\Lambda$  behaves like a cosmological constant in the current Universe. In Ref.[44], the high plateau drives inflation in the early Universe, in which case  $\gamma = \ln(\frac{H_{inf}}{H_\Lambda}) \gg 1$ .

Here, the AdS-EDE model with potential (4) will be briefly called  $\alpha$ AdS. Initially,  $\rho_{\phi_i} = V(\phi_i) \simeq (0.1\text{eV})^4$ , roughly equal to height of the high plateau  $e^{2\gamma}V_0$  if  $\alpha \ll 1$ . In the MCMC analysis, we choose  $6\alpha = (0.15)^2 \ll 1$  for simplicity, thus only  $V_0$ ,  $\gamma$ ,  $V_\Lambda$  are free parameters. The minima of potential (4) is  $V_{min} = -V_0 + V_\Lambda$  at  $\phi = 0$ . Whether potential (4) accommodates AdS vacua or not depends on the value of  $\gamma$ . The existence of an AdS phase requires  $V_0 \gtrsim V_\Lambda$ , i.e.

$$\gamma \lesssim \frac{1}{2} \ln \frac{V(\phi_i)}{V_\Lambda} \simeq 13, \quad (5)$$

where  $V_\Lambda \sim (10^{-4}\text{eV})^4$  is the current dark energy scale. In the limit of large  $\gamma$ , the  $\alpha$ AdS model reduces to a run-away model [15, 16] with  $V(\phi > 0) \sim V_\Lambda$ .

### III. $T_0$ CENSORSHIP OF BEYOND- $\Lambda$ CDM MODELS

#### A. Dataset

Our datasets consist of the Planck18 high- $l$  and low- $l$  TT,EE,TE and lensing likelihoods (P18) [7], the BOSS DR12 [45] with its full covariant matrix for BAO measurements as well as the 6dFGS [46] and MGS of SDSS [47] for low- $z$  BAO, and the Pantheon data (SN) [48]. Recent SH0ES result  $H_0 = 74.03 \pm 1.42\text{km/s/Mpc}$  [4] is employed as a Gaussian prior ( $H_0$ ). We modified the Montepython-3.3 [49, 50] and CLASS [51, 52] codes to perform the MCMC analysis.

Here, we regard  $T_0$  as an MCMC parameter. We sample the cosmological parameter set  $\{\hat{T}_0^{-3}\omega_b, \hat{T}_0^{-3}\omega_{cdm}, H_0, \ln(10^{10}A_s\hat{T}_0^{1+n_s}), n_s, \tau_{reio}, T_0\}$  for  $\Lambda$ CDM, where  $\hat{T}_0 \equiv T_0/T_{0,FIRAS}$  and  $\bar{\omega}_{b/cdm}T_{0,FIRAS}^3 \equiv \hat{T}_0^{-3}\omega_{b/cdm}$  (reducing degeneracy between  $H_0$ ,  $\omega_{b/cdm}$  and  $T_0$ , see Ref.[36]).

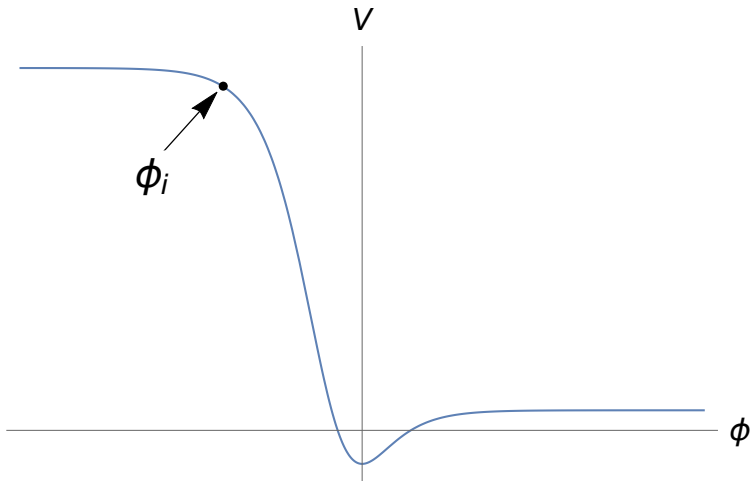


FIG. 1: Potential (4), plotted only for illustration. The scalar field initially sits at  $\phi_i$  near the high plateau. It begins rolling down the potential around matter-radiation equality, passing through the AdS region near  $\phi \simeq 0$  and finally climbs up the low plateau responsible for the current dark energy.

	$100\omega_b\hat{T}^{-3}$	$\omega_{cdm}\hat{T}^{-3}$	$H_0$	$T_0$	$w$	$r_s$
$\Lambda$ CDM+P18	$2.195^{+0.016}_{-0.018}$	$0.1186^{+0.0016}_{-0.0016}$	$69.2^{+2.2}_{-2.3}$	$2.661^{+0.059}_{-0.06}$	-1	$148.4^{+3.3}_{-3.7}$
$\Lambda$ CDM+P18+BAO	$2.189^{+0.014}_{-0.015}$	$0.1194^{+0.0011}_{-0.0011}$	$67.68^{+0.5}_{-0.5}$	$2.701^{+0.016}_{-0.016}$	-1	$146^{+0.8}_{-0.78}$
$\phi^4$	$2.227^{+0.019}_{-0.019}$	$0.1285^{+0.0043}_{-0.0042}$	$70.94^{+1}_{-1.1}$	$2.709^{+0.015}_{-0.016}$	-1	$140.5^{+2.1}_{-2.3}$
$\phi^4$ AdS	$2.296^{+0.017}_{-0.018}$	$0.1344^{+0.0019}_{-0.0022}$	$72.6^{+0.53}_{-0.6}$	$2.716^{+0.016}_{-0.015}$	-1	$136.9^{+1.1}_{-0.91}$
$\alpha$ AdS	$2.273^{+0.044}_{-0.047}$	$0.1345^{+0.002}_{-0.0025}$	$72.57^{+0.52}_{-0.53}$	$2.709^{+0.015}_{-0.016}$	-1	$136.8^{+0.95}_{-0.78}$
$w$ CDM+P18	$2.191^{+0.017}_{-0.017}$	$0.1192^{+0.0015}_{-0.0016}$	$74.42^{+5.6}_{-1.8}$	$2.715^{+0.064}_{-0.071}$	$-1.244^{+0.2}_{-0.16}$	$145.3^{+3.8}_{-3.9}$
$w$ CDM+P18+ $\theta_{BAO}^\perp+H_0$	$2.184^{+0.015}_{-0.015}$	$0.1201^{+0.0011}_{-0.0012}$	$74.01^{+1.4}_{-1.5}$	$2.77^{+0.027}_{-0.025}$	$-1.322^{+0.095}_{-0.084}$	$142.2^{+1.3}_{-1.4}$

TABLE I: Mean and  $1\sigma$  results of all the chains. All EDE models ( $\phi^4$  [14],  $\phi^4$ AdS [20],  $\alpha$ AdS) are confronted with P18+BAO+SN+ $H_0$  datasets.

The  $w$ CDM models introduce one more MCMC parameter  $w$ . Beyond that, the EDE-like models have additional parameters  $\{\omega_{scf}, \ln(1+z_c)\}$ . As described in Refs.[13, 14, 20],  $z_c$  is the redshift at which the field  $\phi$  starts rolling and  $\omega_{scf} = \rho_\phi/\rho_{tot}$  is the energy fraction of EDE at  $z_c$ . Moreover, the  $\alpha$ AdS model (4) has yet a parameter  $\gamma$ . Note that by varying  $\gamma$ , and thus the AdS depth (which was fixed by hand in Ref.[20]), we can explore both the AdS and non-AdS potentials in one MCMC run. Once  $\{\omega_{scf}, \ln(1+z_c), \gamma\}$  are fixed,  $V_\Lambda$  will

be set by matching the budget equation  $\Omega_{DE} = 1 - \Omega_m - \Omega_r$ . The field initially sits around the high plateau  $3\omega_{scf}M_p^2H^2(z_c) \sim e^{2\gamma}V_0$ , so the minimal value  $V_{min}$  of potential (4)

$$V_{min} \sim -3\omega_{scf}M_p^2H^2(z_c)e^{-2\gamma} + V_\Lambda \quad (6)$$

is roughly set by  $\gamma$ ,  $\omega_{scf}$  and  $z_c$ . When  $\gamma \lesssim 13$ ,  $V_{min} < 0$  is AdS-like, see (5).

## B. Physical consideration

In our dataset, CMB and BAO play significant roles. Thus it is worthwhile to highlight their constraints on parameters  $\{h_0, T_0, |w|, \bar{\omega}_m\}$ , where  $h_0 = H_0 \times (100\text{km/s/Mpc})^{-1}$ , which helps to clarify the MCMC results in Sect-III C.

We assume a spatially-flat Universe, which is  $w$ CDM-like after recombination. We can Taylor expand  $D_A(z_{rec})$  around a best-fit Planck  $\Lambda$ CDM model (by performing partial derivatives with respect to one of  $\{h_0, T_0, |w|, \bar{\omega}_m\}$ ) to estimate its dependence on  $\{h_0, T_0, |w|, \bar{\omega}_m\}$ . Using  $\Omega_m \simeq 0.3$  and  $\Omega_{DE} \simeq 0.7$ , for fixed  $\theta_{CMB}$  in (2), we have

$$(r_s T_0) h_0^{0.19} T_0^{0.21} |w|^{-0.09} \bar{\omega}_m^{0.4} = \text{const.} \quad (7)$$

The BOSS experiment [45] sets the BAO angular scales as

$$\theta_{BAO}^{\parallel} = r_d H(z_{eff}) / (1 + z_{eff}), \quad \theta_{BAO}^{\perp} = \frac{r_d}{D_A(z_{eff})}, \quad (8)$$

where  $z_{eff}$  is the effective redshift bins of BOSS DR12 data (i.e.  $z_{eff} = 0.38, 0.51, 0.61$  [45]), and  $r_d$  is the comoving sound horizon at the baryon drag epoch. Here, we take  $z_{eff} = 0.61$  (the results at different  $z_{eff}$  only exhibit slight difference). And for fixed  $\theta_{BAO}^{\parallel}$  and  $\theta_{BAO}^{\perp}$ , we have

$$\theta_{BAO}^{\parallel} : (r_d T_0) h_0^{0.51} T_0^{-0.27} |w|^{-0.26} \bar{\omega}_m^{0.24} = \text{const.} \quad (9)$$

$$\theta_{BAO}^{\perp} : (r_d T_0) h_0^{0.75} T_0^{-0.63} |w|^{-0.17} \bar{\omega}_m^{0.12} = \text{const.} \quad (10)$$

## C. $T_0$ - $H_0$ in MCMC results

Table-I presents the MCMC results for  $\Lambda$ CDM and beyond- $\Lambda$ CDM models, see also the corresponding  $T_0$ - $H_0$  contours in Fig-2. In Appendix-A, we also focus on the  $\alpha$ AdS model, and present the posterior distributions and marginalized contours of all the cosmological

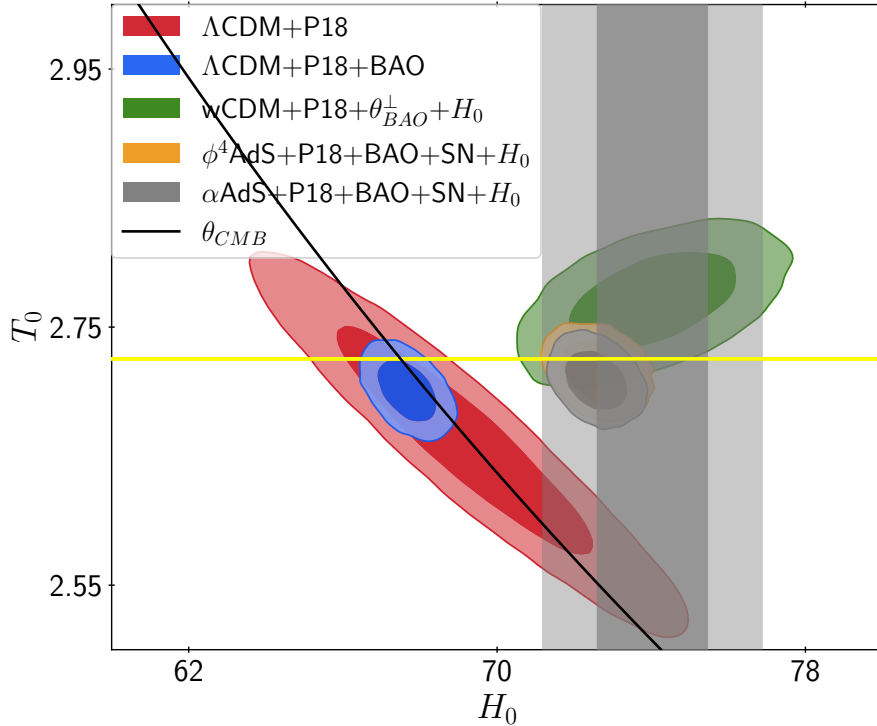


FIG. 2: Marginalized  $1\sigma$  and  $2\sigma$  contours in the  $T_0$ - $H_0$  plane. The gray band is the  $1\sigma$  and  $2\sigma$  SH0ES result  $H_0 = 74.03 \pm 1.42 \text{ km/s/Mpc}$  [4]. The thick yellow line depicts the FIRAS  $1\sigma$  region (1) [33, 34]. Only the EDE models simultaneously lift  $H_0$  and remain compatible with  $T_{0,FIRAS}$ .

parameters and the best-fit  $\chi^2$  values per experiment. As expected, the existence of an AdS phase near recombination can effectively lift  $H_0$  to  $\sim 73 \text{ km/s/Mpc}$  at  $1\sigma$  region.

It is well-known that certain cosmological parameters in EDE models show notable shift from those of the concordance  $\Lambda\text{CDM}$  model. Such parameters may receive additional constraints from the inclusion of new datasets not only depending on  $H_0$ . To further verify the robustness of treating local  $H_0$  measurement as a simple prior, in Appendix-B, we replace the SH0ES prior with the full likelihood code<sup>1</sup> from the H0LiCOW group, which constrains the time delay distance  $D_{\Delta t}$  and/or angular diameter distance to lens  $D_d$  of six strong gravitational lenses. We confirm that using the full likelihood yields results nearly identical to those using the Gaussian prior.

<sup>1</sup> written by Stefan Taubenberger and Sherry Suyu, available at <https://zenodo.org/record/3632967#.X2nuiUBuJ9B>

In Fig-2, we see that the  $\Lambda$ CDM+P18 contour respects Eq.(7) (the  $\theta_{CMB}$  line). The  $\Lambda$ CDM+P18 contour intersects with the SH0ES band at  $T_0 \sim 2.6K$ , which is inconsistent with  $T_{0,FIRAS}$ . As has been pointed out in Ref.[36],  $T_0$  yielded by the Planck and SH0ES data has  $> 4\sigma$  discrepancy compared with  $T_{0,FIRAS}$ .

However, the EDE scenario not only lifts  $H_0$ , but also is compatible with  $T_{0,FIRAS}$ . This can be explained as follows. In CMB and BAO constraints (7), (9) and (10), we have  $|w| = 1$  for EDE scenarios. The Universe after recombination is  $\Lambda$ CDM-like, and  $r_d \sim r_s$ , since the physics at and after recombination must not be affected by EDE. Thus we (approximately) solve Eqs.(7), (9) and (10) for  $T_0 = T_{0,FIRAS}$ , and have

$$r_s h_0 \simeq const., \quad \bar{\omega}_m^{-1} h_0^2 \simeq const. \quad (11)$$

Thus though  $h_0$  is lifted due to  $h_0 \sim r_s^{-1}$  (essence of the EDE idea),  $T_0 = T_{0,FIRAS}$  needs not to be shifted. The expense of compatibility with  $T_{0,FIRAS}$  is that

$$\bar{\omega}_m = \left( \frac{h_0^2}{h_{0,\Lambda}^2} \right) \bar{\omega}_{m,\Lambda CDM} \quad (12)$$

must be magnified. According to (12), we actually have  $\Omega_m \simeq const$  (equivalently  $\Omega_m \simeq \Omega_{m,\Lambda CDM}$ ), since  $\omega_m = \Omega_m h_0^2$ . It is worth mentioning that the  $\Omega_m \sim const.$  constraint is applicable to any mechanism that modifies the sound horizon around recombination with a  $\Lambda$ CDM-like universe after that, not necessarily EDE. As a consistency check of (12), for  $h_{0,\Lambda CDM} \sim 0.68$  and  $\bar{\omega}_{m,\Lambda CDM} \sim 0.14$  in  $\Lambda$ CDM (see Table-I), we will have  $\bar{\omega}_m \sim 0.16$  in AdS-EDE models ( $h_0 \sim 0.73$ ), consistent with the results in Table-I. We plot contours of  $\{H_0, T_0, \bar{\omega}_m\}$  in Fig-3. As expected,  $H_0$  is lifted respecting Eq.(12).

In  $\Lambda$ CDM,  $\omega_m$  is difficult to adjust since it is well constrained by Planck, but in EDE  $\omega_m$  can be consistently tuned due to the scalar field perturbations, see Appendix-C. This seems to cause a slightly larger  $\sigma_8$ , so-called  $S_8$  tension, e.g.[53], see also [54–56]. However, this tension is also present in  $\Lambda$ CDM with  $\sim 2\sigma$  significance (inherited but not significantly exacerbated in EDE, as argued in [22, 57]), which might be related with systematic error or possible intrinsic inconsistency of Planck data itself [58, 59].

The low- $z$  resolutions beyond  $\Lambda$ CDM have been also studied in e.g.[27, 60–67]. It is usually thought that  $w$ CDM models with  $w \simeq -1.3$  might resolve the Hubble tension, e.g.[39, 60, 68], though it is disfavored by the full BAO data. However, in Fig-2, we see that such a solution seems also incompatible with  $T_{0,FIRAS}$ .



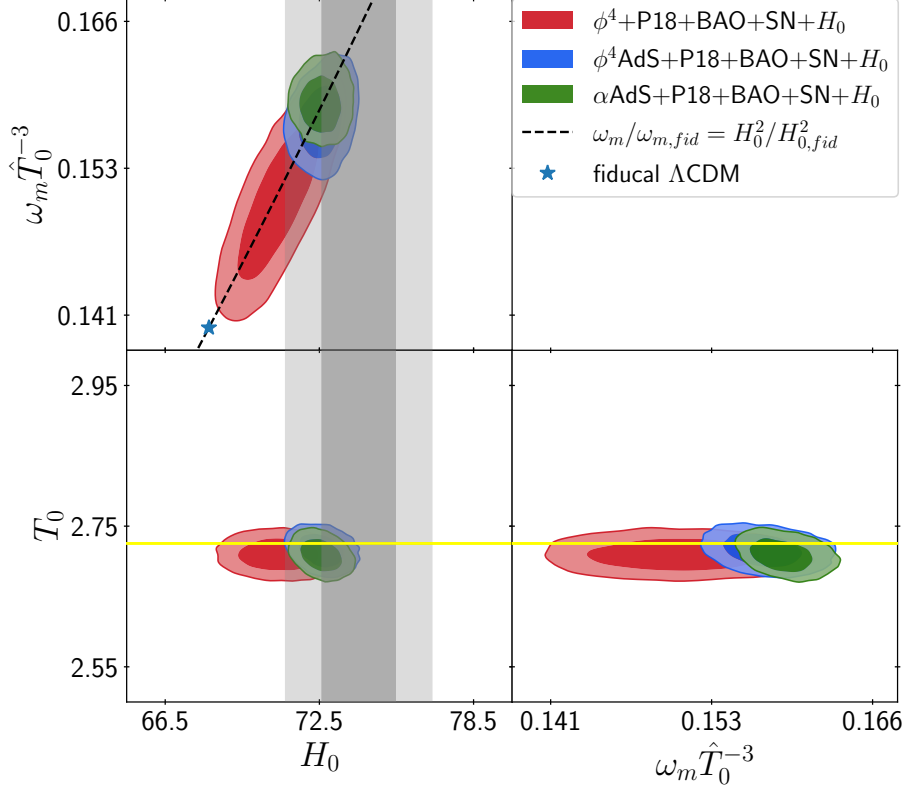


FIG. 3: Marginalized  $1\sigma$  and  $2\sigma$  contours of the EDE models in the  $\{T_0 - \bar{\omega}_m - H_0\}$  space.  $T_{0,FIRAS}$  and  $H_0$  are plotted as described in Fig-2. The  $\omega_m \hat{T}_0^{-3} - H_0$  contours of all EDE models respect Eq.(12) (dashed line).

The  $w$ CDM model, like  $\Lambda$ CDM, does not alter the physics around and before recombination, so  $r_s T_0$  is constant [36]. It is well-known that  $w$ CDM with  $w < -1$  is not supported by the full BAO data, e.g.recent Ref.[68], so we only solve Eqs.(7) and (10), and have

$$h_0^{-3}|w| \simeq const., \quad T_0^{-8}|w| \simeq const. \quad (13)$$

Note (13) is conflicted with BAO constraint (9), see the black line in Fig-4. Here, if  $|w| > 1$ ,  $h_0 \propto |w|^{1/3}$  will be lifted. However,  $T_0 \propto |w|^{1/8}$  must also be magnified, which will make  $T_0$  inconsistent with the result (1) of  $T_{0,FIRAS}$ . Though we can fix  $T_0 = T_{0,FIRAS}$ , and have  $h_0 \sim |w|^{9/19}$  for the CMB constraint (7), it is obviously conflicted with BAO constraints (9) and (10). As a consistency check of (13), for  $h_0 \sim 0.68$  in  $\Lambda$ CDM, we will have  $w \simeq -1.3$  in

$w$ CDM ( $h_0 \sim 0.74$ ) but

$$T_0 \simeq T_{0,FIRAS}|w|^{1/8} \sim 2.8K, \quad (14)$$

which is consistent with the  $w$ CDM results in Table-I. Here, we confront  $w$ CDM with P18 and perpendicular BAO data ( $\theta_{BAO}^\perp$ ). The contours of  $\{H_0, T_0, w\}$  is plotted in Fig-4, which clearly shows the inconsistency of  $w$ CDM with  $T_{0,FIRAS}$ . As expected,  $T_0$  is lifted respecting Eq.(14).

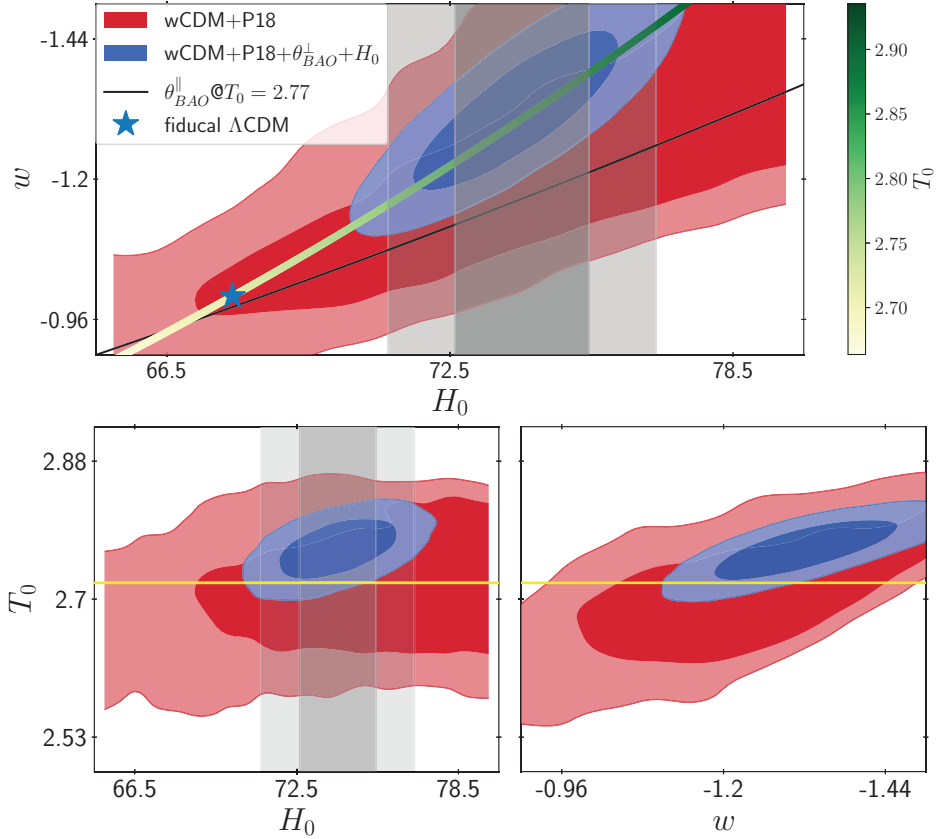


FIG. 4: Marginalized  $1\sigma$  and  $2\sigma$  contours of the  $w$ CDM model in the  $\{w-T_0-H_0\}$  space.  $T_{0,FIRAS}$  and  $H_0$  are plotted as described in Fig-2. Upper panel: The rainbow line plots compatible intersections of (7) and (10) at different  $T_0$ , with a color coding for  $T_0$ . As expected, the contour of the  $w$ CDM model spreads along the predicted line. The black line plots the  $\theta_{BAO}^\parallel$  constraint (9) at  $T_0 = 2.77K$  (see Table-I), which suggests that  $w$ CDM with  $w \lesssim -1.3$  is not actually favored by BAO data. Lower Panel: In addition, such a  $w$ CDM model is also inconsistent with  $T_{0,FIRAS}$ .

#### IV. CONCLUSION

It is well-known that  $H_0$  and  $T_0$  are basic cosmological parameters (specially not dimensionless). Precisely measured value  $T_{0,FIRAS}$  of  $T_0$  can be regarded as a censorship of beyond- $\Lambda$ CDM models resolving the  $H_0$  tension.

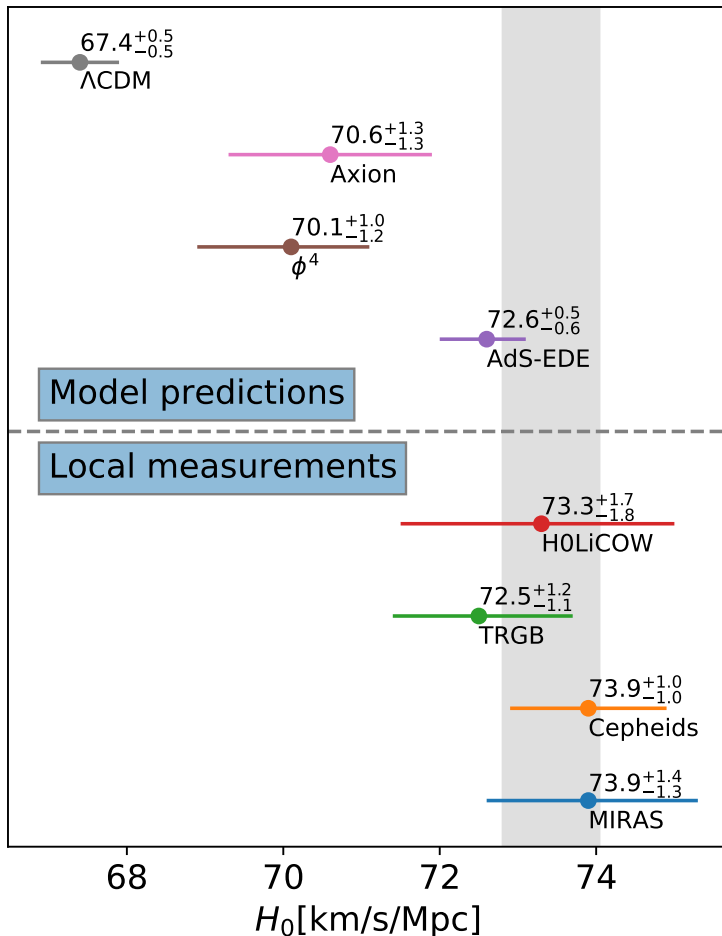


FIG. 5: Predicted  $H_0$  values in the  $\Lambda$ CDM, axion-like [13],  $\phi^4$  [14] and AdS-EDE models confronted with various mutually independent local measurements. MIRAS, Cepheids and TRGB stands for three independent Type Ia supernova calibrators in the local distance ladder (see Ref.[8]). The  $H_0$  measured by lensing time delays from lensed quasars, independent of the distance ladder approach, is also included (the H0LiCOW result [1]). Gray band represents the combined  $1\sigma$  region of the measured  $H_0$ .

We, based on Eqs.(7), (9) and (10) (i.e. CMB and BAO constraints), identified why EDE is compatible with  $T_{0,FIRAS}$ , while lifting  $H_0$  at the cost of an enhanced  $\omega_m$ . As a contrast, we also showed that  $w$ CDM models with  $w \lesssim -1.3$  seem inconsistent with  $T_{0,FIRAS}$ . We performed MCMC analysis for the corresponding models to confirm our observations. It has been pointed out in Ref.[36] that for  $\Lambda$ CDM,  $T_0$  yielded by the Planck and SH0ES data has  $> 4\sigma$  discrepancy compared with  $T_{0,FIRAS}$ . However, we showed that EDE is compatible with not only  $T_{0,FIRAS}$ , but also known independent local measurements of  $H_0$ , see Fig-5 and Appendix-B. As argued in section-III B,  $H_0$  is lifted at the cost of an enlarged  $\omega_m$  and also an enhanced  $n_s$  compensating for diffusion damping at high  $l$ , the corresponding models are thus expected to receive tight constraints with the inclusion of matter power spectrum data [54–56], which will be left for future study. Still, our result suggests that even if EDE is not the final story restoring cosmological concordance, it might be on the right road and relevant issues are worth studying.

Inspired by the  $\alpha$ -attractor [43, 44], we also presented a well-motivated AdS-EDE model. In the MCMC analysis, we do not assume AdS *in priori*, but in Fig-6 we see that the MCMC result weakly hints the existence of an AdS phase, with the best-fit cosmology having AdS depth  $V_{min} \sim -(0.001\text{eV})^4$ . The best-fit model allows  $H_0 \sim 73\text{km/s/Mpc}$  at  $1\sigma$  range, which indicates that the existence of AdS phase around recombination helps to significantly lift  $H_0$ . Our result again highlights an unexpected point that AdS vacua, ubiquitous in consistent UV-complete theories, might also play a crucial role in our observable Universe.

*Acknowledgments* This work is supported by the University of Chinese Academy of Sciences. Y.S.P. is supported by NSFC, Nos. 11575188, 11690021. The computations are performed on the TianHe-II supercomputer.

## Appendix A: MCMC results of the $\alpha$ AdS model

In the MCMC analysis we sample over  $\{\omega_b/\hat{T}_0^3, \omega_{cdm}/\hat{T}_0^3, H_0, \ln(10^{10} A_s \hat{T}_0^{1+n_s}), n_s, \tau_{reio}, T_0, \omega_{scf}, \ln(1+z_c), \gamma\}$ . We use flat priors for additional EDE parameters (Table-II). Here, we do not assume AdS *in priori* in the MCMC analysis, since the  $\gamma$  prior in Table-II covers non-AdS region of the potential, see Eq.(5). Posterior distributions and marginalized contours of all cosmological parameters are plotted in Fig-7. The mean and best-fit values are shown in Table-III. We also report the best-fit  $\chi^2$  values per experiment in Table-IV.

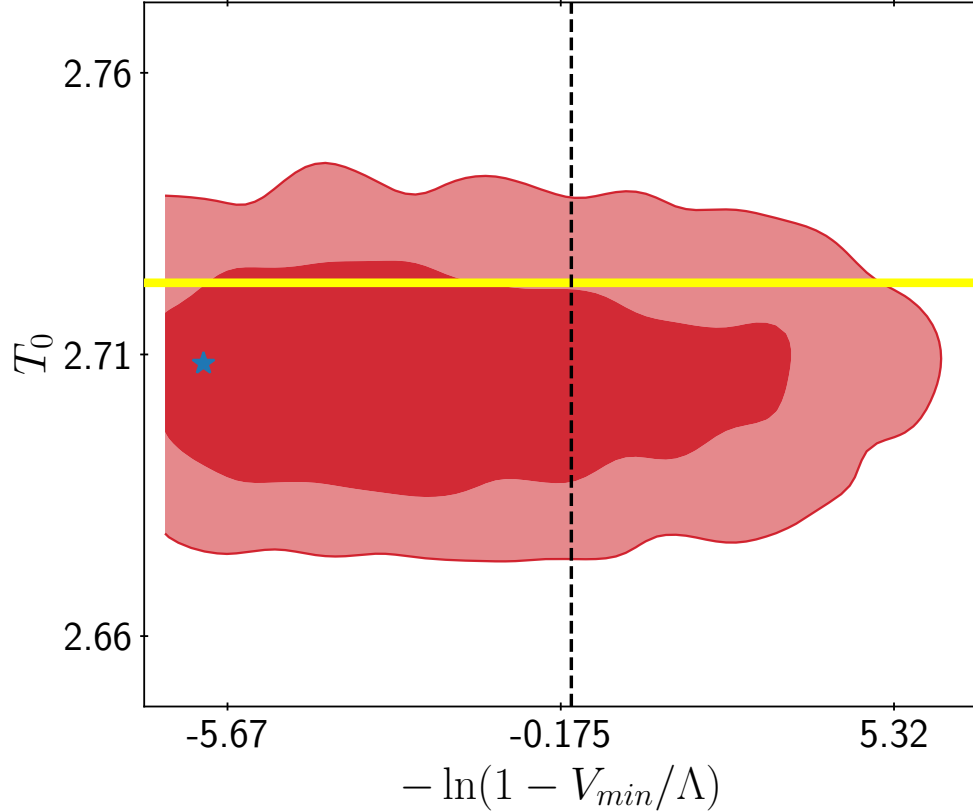


FIG. 6: Marginalized contour of  $T_0$  with respect to  $V_{min}/\Lambda$ . The axis  $-\ln(1 - V_{min}/\Lambda)$  is chosen such that it is log scale when  $-V_{min}/\Lambda \ll 1$  (deep in the AdS phase) and  $V_{min}/\Lambda \rightarrow 1$ , while it is linear around  $V_{min} \sim 0$ . Dashed line labels  $V_{min} = 0$ . Yellow band represents  $T_{0,FIRAS}$ .

TABLE II: Flat priors of  $\alpha$ AdS parameters

	prior
$\omega_{scf}$	$[10^{-4}, 0.4]$
$\ln(1 + z_c)$	$[7.5, 9.5]$
$\gamma$	$[5, 15]$

## Appendix B: MCMC results including the lensing time delay measurements

All MCMC analyses presented in the main text employ the SH0ES result as a Gaussian prior, it is thus worth checking if the results are compatible with other independent experiments. The current  $H_0$  can be measured by lensing time delays of strongly lensed quasar images, completely independent of the local distance ladder approach, in particular

TABLE III: Mean and best-fit values of all model parameters

Param	best-fit	mean $\pm\sigma$	95% lower	95% upper
$100\omega_b\hat{T}_0^{-3}$	2.278	$2.273_{-0.047}^{+0.044}$	2.182	2.365
$\omega_{cdm}\hat{T}_0^{-3}$	0.1333	$0.1345_{-0.0025}^{+0.002}$	0.1302	0.1391
$H_0$	72.54	$72.57_{-0.53}^{+0.52}$	71.56	73.63
$\ln(10^{10}A_s\hat{T}_0^{1+n_s})$	3.076	$3.077_{-0.015}^{+0.016}$	3.046	3.108
$n_s$	0.9939	$0.9926_{-0.0044}^{+0.0043}$	0.9839	1.001
$\ln(1+z_c)$	8.479	$8.51_{-0.061}^{+0.076}$	8.362	8.651
$\omega_{scf}$	0.1091	$0.1098_{-0.002}^{+0.0006}$	0.1073	0.1134
$\gamma$	8.748	$10.98_{-2.2}^{+1}$	8.444	13.92
$T_0$	2.711	$2.709_{-0.016}^{+0.015}$	2.679	2.74
$\sigma_8$	0.8635	$0.8677_{-0.012}^{+0.012}$	0.8435	0.8922

TABLE IV: best-fit  $\chi^2$  per experiment

Experiment	$\chi^2$
Planck high $l$	2347.44
Planck low $l$	416.89
Planck lensing	11.79
BAO BOSS DR12	0.66
BAO low $z$	2.46
Pantheon	1026.94
SH0ES	1.33

SH0ES. To this end we re-analyze the  $\alpha$ AdS model (4) with the same ten model parameters as discussed in the main text and the dataset P18+BAO+SN+H0LiCOW. In Fig-8 we plot relevant  $T_0 - H_0$  contours and posterior distributions. We also include a combining all (H0LiCOW+SH0ES) result since the two datasets are independent of each other. It is clear that the MCMC analysis with the full H0LiCOW likelihood code yields nearly identical results to that with the SH0ES prior, confirming the robustness of treating local

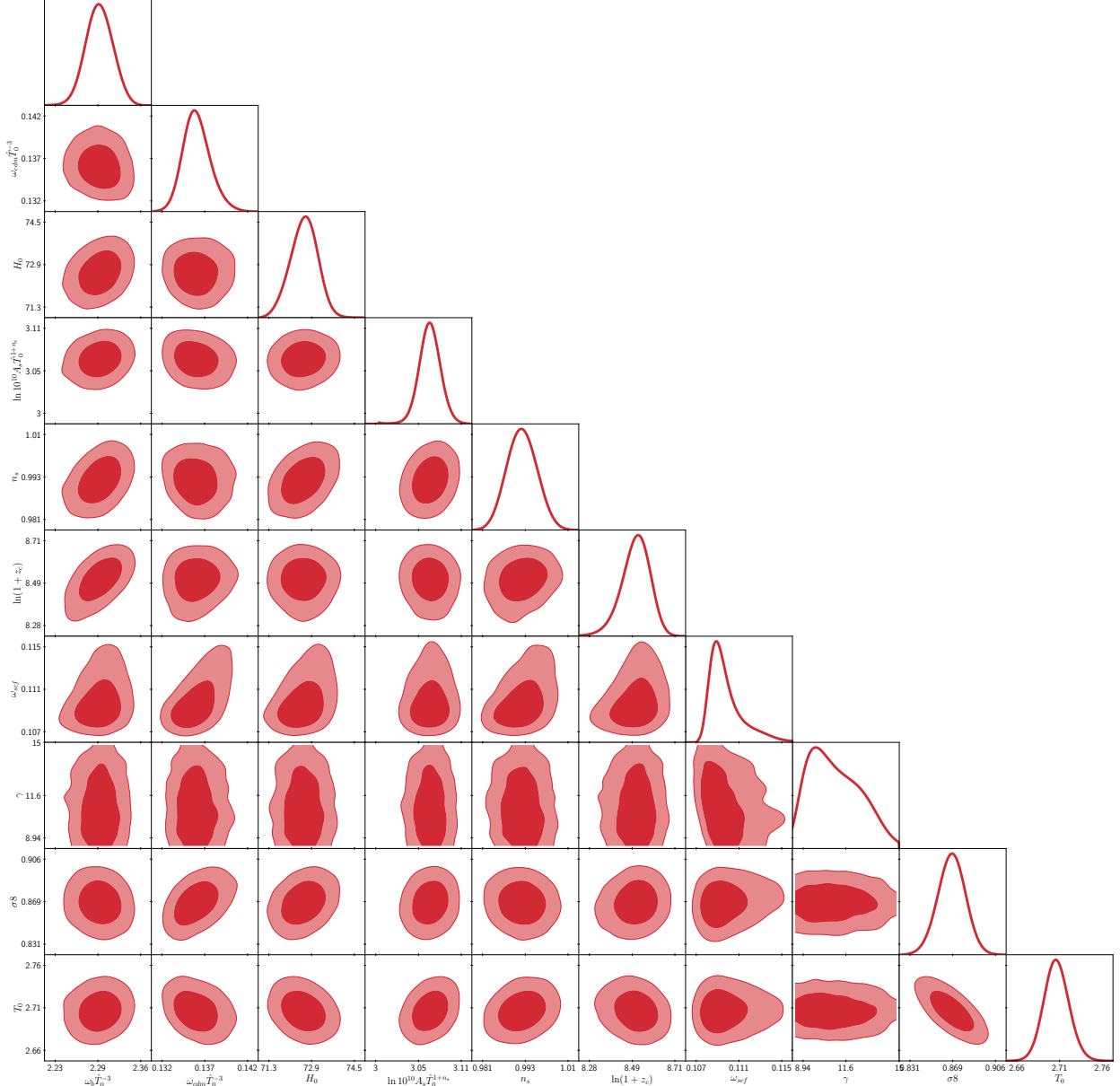


FIG. 7: Posterior distributions and marginalized 68% and 95% contours of all model parameters in the  $\alpha$ AdS model confronted with the full datasets P18+BAO+SN+ $H_0$ .

$H_0$  measurements as simple Gaussian priors in the MCMC analysis<sup>2</sup>. Additionally, we vary  $H_0$ , for each of the six lenses in H0LiCOW, with all other parameters fixed at their best-fit values in  $\alpha$ AdS and plot the results in Fig-9. Ref.[1] noted a possible trend (not yet sta-

<sup>2</sup> The mean  $H_0$  predicted by the P18+BAO+SN+H0LiCOW chain is slightly smaller than that of the SH0ES chain. The SH0ES prior also seems to dominate over the H0LiCOW data in the combining all chain. We attribute this to the larger mean value and shorter error bar of  $H_0$  in the SH0ES measurement.

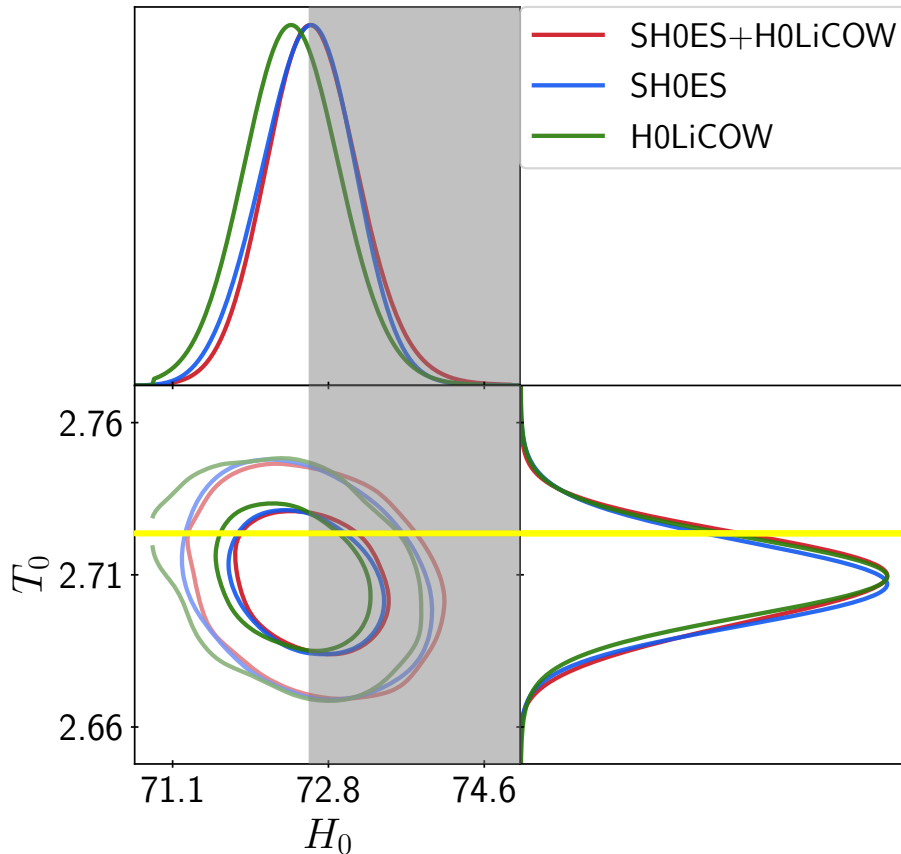


FIG. 8: Posterior distributions and 68% and 95% contours of  $T_0$  and  $H_0$  in the  $\alpha$ AdS model confronted with P18+BAO+SN+SH0ES/H0LiCOW and P18+BAO+SN+SH0ES+H0LiCOW. The gray (yellow) band corresponds to the  $1\sigma$  region of the SH0ES (FIRAS) measurement.

tistically significant due to the small sample size) of lower lens redshift systems having a larger inferred value of  $H_0$ . Fig-9 shows such a trend, if really exists, seems to persist in the AdS-EDE model.

### Appendix C: Scalar field perturbations in EDE and $\omega_m$

When the EDE becomes non-negligible, the gravitational perturbation  $\Psi$  will be suppressed by the EDE perturbations [54]. In order to preserve the fit to the CMB data,  $\omega_m$  must increase accordingly to compensate for the slight suppress in  $\Psi$ .

We plot the evolution of  $\Psi$  in Fig-10. Two EDE lines are nearly identical at high- $z$  due



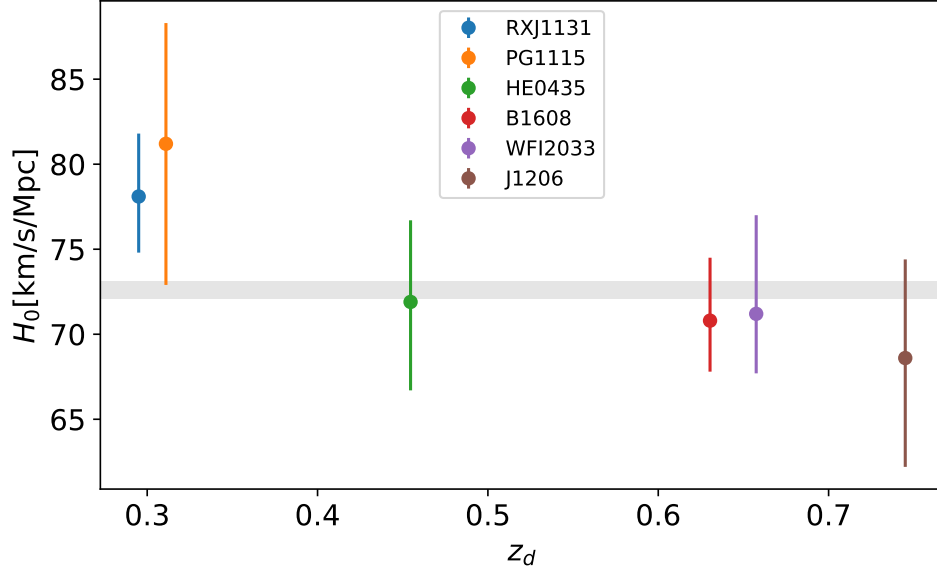


FIG. 9: Measured values of  $H_0$  per lens of H0LiCOW versus lens redshift  $z_d$  in the best-fit  $\alpha$ AdS model. The lenses presented are B1608 [69, 70], HE0435 [71, 72], J1206 [73], RXJ1131 [72, 74], PG1115 [72] and WFI2033 [75].

to the same cosmological parameters except for  $\omega_{cdm}$ . However, they will not coincide any longer when EDE becomes non-negligible.  $\Psi$  in the  $\phi^4$ AdS model with fixed  $\omega_{cdm} = 0.122$  is suppressed compared with that in the best-fit  $\phi^4$ AdS model. This is because in the best-fit  $\phi^4$ AdS model such suppression will be compensated by the gravity of extra dark matter abundance, which lifts  $\Psi$  at recombination to the  $\Lambda$ CDM value (dashed line), so produces correct power in the CMB TT spectrum.

- 
- [1] K. C. Wong, S. H. Suyu, G. C. F. Chen, C. E. Rusu, M. Millon, D. Sluse, V. Bonvin, C. D. Fassnacht, S. Taubenberger, M. W. Auger, S. Birrer, J. H. Chan, F. Courbin, S. Hilbert, O. Tihhonova, T. Treu, A. Agnello, X. Ding, I. Jee, E. Komatsu, A. J. Shajib, A. Sonnenfeld, R. D. Blandford, L. V. Koopmans, P. J. Marshall and G. Meylan, [arXiv:1907.04869 [astro-ph.CO]].
- [2] W. L. Freedman, B. F. Madore, D. Hatt, T. J. Hoyt, I. S. Jang, R. L. Beaton, C. R. Burns, M. G. Lee, A. J. Monson, J. R. Neeley, M. M. Phillips, J. A. Rich and M. Seibert,

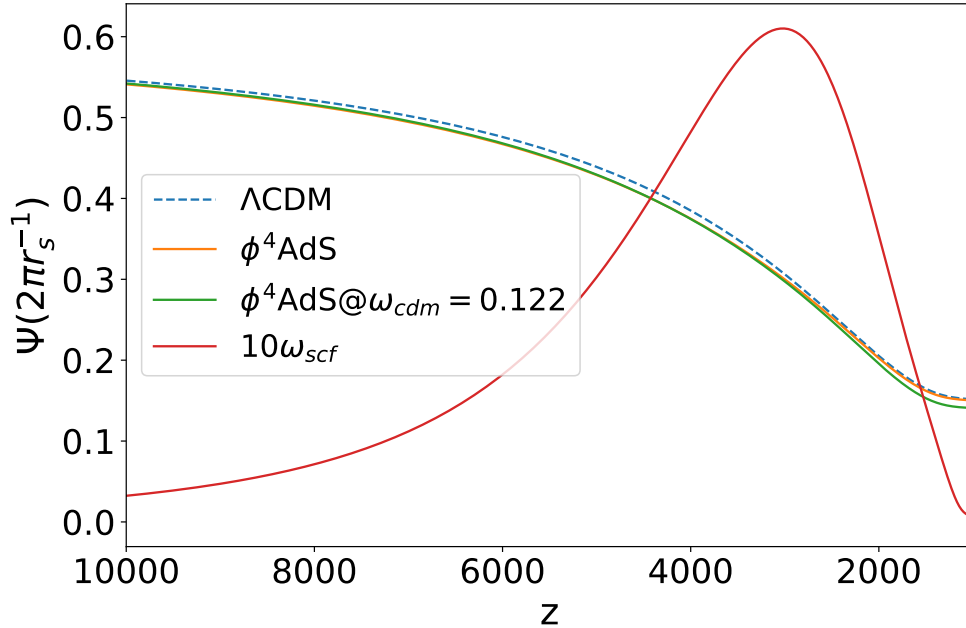


FIG. 10: Evolution of  $\Psi$  with  $k = 2\pi/r_s$ , which roughly corresponds to the first acoustic peak, plotted for the best-fit models of  $\Lambda$ CDM and  $\phi^4$ AdS. The green line is produced by a  $\phi^4$ AdS model with reduced  $\omega_{cdm}$  while fixing all other parameters to the best-fit.

[arXiv:1907.05922 [astro-ph.CO]].

- [3] C. D. Huang, A. G. Riess, W. Yuan, L. M. Macri, N. L. Zakamska, S. Casertano, P. A. Whitelock, S. L. Hoffmann, A. V. Filippenko and D. Scolnic, [arXiv:1908.10883 [astro-ph.CO]].
- [4] A. G. Riess, S. Casertano, W. Yuan, L. M. Macri and D. Scolnic, *Astrophys. J.* **876**, no.1, 85 (2019) [arXiv:1903.07603 [astro-ph.CO]].
- [5] A. G. Riess, W. Yuan, S. Casertano, L. M. Macri and D. Scolnic, [arXiv:2005.02445 [astro-ph.CO]].
- [6] A. G. Riess, *Nature Rev. Phys.* **2**, no. 1, 10 (2019) [arXiv:2001.03624 [astro-ph.CO]].
- [7] N. Aghanim *et al.* [Planck], [arXiv:1807.06209 [astro-ph.CO]].
- [8] L. Verde, T. Treu and A. Riess, [arXiv:1907.10625 [astro-ph.CO]].
- [9] J. L. Bernal, L. Verde and A. G. Riess, *JCAP* **1610**, 019 (2016) [arXiv:1607.05617 [astro-ph.CO]].
- [10] K. Aylor, M. Joy, L. Knox, M. Millea, S. Raghunathan and W. K. Wu, *Astrophys. J.* **874**, no.1, 4 (2019) [arXiv:1811.00537 [astro-ph.CO]].
- [11] L. Knox and M. Millea, *Phys. Rev. D* **101**, no.4, 043533 (2020) [arXiv:1908.03663 [astro-

- ph.CO]].
- [12] M. Z. Lyu, B. S. Haridasu, M. Viel and J. Q. Xia, [arXiv:2001.08713 [astro-ph.CO]].
  - [13] V. Poulin, T. L. Smith, T. Karwal and M. Kamionkowski, Phys. Rev. Lett. **122**, no.22, 221301 (2019) [arXiv:1811.04083 [astro-ph.CO]].
  - [14] P. Agrawal, F. Y. Cyr-Racine, D. Pinner and L. Randall, [arXiv:1904.01016 [astro-ph.CO]].
  - [15] S. Alexander and E. McDonough, Phys. Lett. B **797**, 134830 (2019) [arXiv:1904.08912 [astro-ph.CO]].
  - [16] M. X. Lin, G. Benevento, W. Hu and M. Raveri, Phys. Rev. D **100**, no.6, 063542 (2019) [arXiv:1905.12618 [astro-ph.CO]].
  - [17] T. L. Smith, V. Poulin and M. A. Amin, Phys. Rev. D **101**, no.6, 063523 (2020) [arXiv:1908.06995 [astro-ph.CO]].
  - [18] F. Niedermann and M. S. Sloth, [arXiv:1910.10739 [astro-ph.CO]].
  - [19] J. Sakstein and M. Trodden, Phys. Rev. Lett. **124**, no.16, 161301 (2020) [arXiv:1911.11760 [astro-ph.CO]].
  - [20] G. Ye and Y. S. Piao, Phys. Rev. D **101**, no.8, 083507 (2020) [arXiv:2001.02451 [astro-ph.CO]].
  - [21] M. Braglia, W. T. Emond, F. Finelli, A. E. Gumrukcuoglu and K. Koyama, [arXiv:2005.14053 [astro-ph.CO]].
  - [22] F. Niedermann and M. S. Sloth, [arXiv:2006.06686 [astro-ph.CO]].
  - [23] G. Ballesteros, A. Notari and F. Rompineve, arXiv:2004.05049 [astro-ph.CO].
  - [24] M. Zumalacarregui, Phys. Rev. D **102**, no. 2, 023523 (2020) [arXiv:2003.06396 [astro-ph.CO]].
  - [25] M. Braglia, M. Ballardini, W. T. Emond, F. Finelli, A. E. Gumrukcuoglu, K. Koyama and D. Paoletti, Phys. Rev. D **102**, no. 2, 023529 (2020) [arXiv:2004.11161 [astro-ph.CO]].
  - [26] L. Visinelli, S. Vagnozzi and U. Danielsson, Symmetry **11**, no.8, 1035 (2019) [arXiv:1907.07953 [astro-ph.CO]].
  - [27] O. Akarsu, J. D. Barrow, L. A. Escamilla and J. A. Vazquez, Phys. Rev. D **101**, no. 6, 063528 (2020) [arXiv:1912.08751 [astro-ph.CO]].
  - [28] R. Calderón, R. Gannouji, B. L’Huillier and D. Polarski, [arXiv:2008.10237 [astro-ph.CO]].
  - [29] H. Ooguri and C. Vafa, Nucl. Phys. B **766**, 21-33 (2007) [arXiv:hep-th/0605264 [hep-th]].
  - [30] G. Obied, H. Ooguri, L. Spodyneiko and C. Vafa, [arXiv:1806.08362 [hep-th]].
  - [31] Y. S. Piao, Phys. Rev. D **70**, 101302 (2004) [hep-th/0407258].
  - [32] H. H. Li, G. Ye, Y. Cai and Y. S. Piao, Phys. Rev. D **101**, no. 6, 063527 (2020)

- [arXiv:1911.06148 [gr-qc]].
- [33] D. Fixsen, E. Cheng, J. Gales, J. C. Mather, R. Shafer and E. Wright, *Astrophys. J.* **473**, 576 (1996) [arXiv:astro-ph/9605054 [astro-ph]].
- [34] D. Fixsen, *Astrophys. J.* **707**, 916-920 (2009) [arXiv:0911.1955 [astro-ph.CO]].
- [35] P. Ade *et al.* [Planck], *Astron. Astrophys.* **594**, A13 (2016) [arXiv:1502.01589 [astro-ph.CO]].
- [36] M. M. Ivanov, Y. Ali-Haïmoud and J. Lesgourgues, [arXiv:2005.10656 [astro-ph.CO]].
- [37] C. A. P. Bengaly, J. E. Gonzalez and J. S. Alcaniz, arXiv:2007.13789 [astro-ph.CO].
- [38] B. Bose and L. Lombriser, arXiv:2006.16149 [astro-ph.CO].
- [39] S. Vagnozzi, *Phys. Rev. D* **102**, no. 2, 023518 (2020) [arXiv:1907.07569 [astro-ph.CO]].
- [40] G. Benevento, W. Hu and M. Raveri, *Phys. Rev. D* **101**, no.10, 103517 (2020) [arXiv:2002.11707 [astro-ph.CO]].
- [41] E. Di Valentino, E. V. Linder and A. Melchiorri, [arXiv:2006.16291 [astro-ph.CO]].
- [42] B. S. Haridasu and M. Viel, arXiv:2004.07709 [astro-ph.CO].
- [43] J. J. M. Carrasco, R. Kallosh and A. Linde, *Phys. Rev. D* **92**, no.6, 063519 (2015) [arXiv:1506.00936 [hep-th]].
- [44] Y. Akrami, R. Kallosh, A. Linde and V. Vardanyan, *JCAP* **06**, 041 (2018) [arXiv:1712.09693 [hep-th]].
- [45] S. Alam *et al.* [BOSS], *Mon. Not. Roy. Astron. Soc.* **470**, no.3, 2617-2652 (2017) [arXiv:1607.03155 [astro-ph.CO]].
- [46] F. Beutler, C. Blake, M. Colless, D. Jones, L. Staveley-Smith, L. Campbell, Q. Parker, W. Saunders and F. Watson, *Mon. Not. Roy. Astron. Soc.* **416**, 3017-3032 (2011) [arXiv:1106.3366 [astro-ph.CO]].
- [47] A. J. Ross, L. Samushia, C. Howlett, W. J. Percival, A. Burden and M. Manera, *Mon. Not. Roy. Astron. Soc.* **449**, no.1, 835-847 (2015) [arXiv:1409.3242 [astro-ph.CO]].
- [48] D. Scolnic, D. Jones, A. Rest, Y. Pan, R. Chornock, R. Foley, M. Huber, R. Kessler, G. Narayan, A. Riess, S. Rodney, E. Berger, D. Brout, P. Challis, M. Drout, D. Finkbeiner, R. Lunnan, R. Kirshner, N. Sanders, E. Schlafly, S. Smartt, C. Stubbs, J. Tonry, W. Wood-Vasey, M. Foley, J. Hand, E. Johnson, W. Burgett, K. Chambers, P. Draper, K. Hodapp, N. Kaiser, R. Kudritzki, E. Magnier, N. Metcalfe, F. Bresolin, E. Gall, R. Kotak, M. McCrum and K. Smith, *Astrophys. J.* **859**, no.2, 101 (2018) [arXiv:1710.00845 [astro-ph.CO]].
- [49] B. Audren, J. Lesgourgues, K. Benabed and S. Prunet, *JCAP* **02**, 001 (2013) [arXiv:1210.7183

- [astro-ph.CO]].
- [50] T. Brinckmann and J. Lesgourgues, *Phys. Dark Univ.* **24**, 100260 (2019) [arXiv:1804.07261 [astro-ph.CO]].
- [51] J. Lesgourgues, [arXiv:1104.2932 [astro-ph.IM]].
- [52] D. Blas, J. Lesgourgues and T. Tram, *JCAP* **07**, 034 (2011) [arXiv:1104.2933 [astro-ph.CO]].
- [53] M. Raveri and W. Hu, *Phys. Rev. D* **99**, no.4, 043506 (2019) [arXiv:1806.04649 [astro-ph.CO]].
- [54] J. C. Hill, E. McDonough, M. W. Toomey and S. Alexander, [arXiv:2003.07355 [astro-ph.CO]].
- [55] M. M. Ivanov, E. McDonough, J. C. Hill, M. Simonović, M. W. Toomey, S. Alexander and M. Zaldarriaga, [arXiv:2006.11235 [astro-ph.CO]].
- [56] G. D’Amico, L. Senatore, P. Zhang and H. Zheng, [arXiv:2006.12420 [astro-ph.CO]].
- [57] A. Klypin, V. Poulin, F. Prada, J. Primack, M. Kamionkowski, V. Avila-Reese, A. Rodriguez-Puebla, P. Behroozi, D. Hellinger and T. L. Smith, [arXiv:2006.14910 [astro-ph.CO]].
- [58] W. L. K. Wu, P. Motloch, W. Hu and M. Raveri, [arXiv:2004.10207 [astro-ph.CO]].
- [59] A. Chudaykin, D. Gorbunov and N. Nedelko, [arXiv:2004.13046 [astro-ph.CO]].
- [60] E. Di Valentino, A. Melchiorri and J. Silk, *Phys. Lett. B* **761**, 242-246 (2016) [arXiv:1606.00634 [astro-ph.CO]].
- [61] E. Di Valentino, A. Melchiorri and O. Mena, *Phys. Rev. D* **96**, no.4, 043503 (2017) [arXiv:1704.08342 [astro-ph.CO]].
- [62] E. Di Valentino, A. Melchiorri, E. V. Linder and J. Silk, *Phys. Rev. D* **96**, no.2, 023523 (2017) [arXiv:1704.00762 [astro-ph.CO]].
- [63] E. Di Valentino, A. Melchiorri, O. Mena and S. Vagnozzi, [arXiv:1908.04281 [astro-ph.CO]].
- [64] S. F. Yan, P. Zhang, J. W. Chen, X. Z. Zhang, Y. F. Cai and E. N. Saridakis, *Phys. Rev. D* **101**, no.12, 121301 (2020) [arXiv:1909.06388 [astro-ph.CO]].
- [65] W. Yang, E. Di Valentino, S. Pan, S. Basilakos and A. Paliathanasis, arXiv:2001.04307 [astro-ph.CO].
- [66] W. Yang, E. Di Valentino, S. Pan and O. Mena, [arXiv:2007.02927 [astro-ph.CO]].
- [67] H. B. Benaoum, W. Yang, S. Pan and E. Di Valentino, arXiv:2008.09098 [gr-qc].
- [68] G. Alestas, L. Kazantzidis and L. Perivolaropoulos, *Phys. Rev. D* **101**, no.12, 123516 (2020) [arXiv:2004.08363 [astro-ph.CO]].
- [69] Suyu, S. H., P. J. Marshall, M. W. Auger, S. Hilbert, R. D. Blandford, L. V. E. Koopmans, C. D. Fassnacht, and T. Treu. *Astrophys. J.* 711, 201-221.

- [70] I. Jee, S. Suyu, E. Komatsu, C. D. Fassnacht, S. Hilbert and L. V. E. Koopmans, [arXiv:1909.06712 [astro-ph.CO]].
- [71] K. C. Wong, S. H. Suyu, M. W. Auger, V. Bonvin, F. Courbin, C. D. Fassnacht, A. Halkola, C. E. Rusu, D. Sluse and A. Sonnenfeld, *et al.* Mon. Not. Roy. Astron. Soc. **465**, no.4, 4895-4913 (2017) [arXiv:1607.01403 [astro-ph.CO]].
- [72] G. C. F. Chen, C. D. Fassnacht, S. H. Suyu, C. E. Rusu, J. H. H. Chan, K. C. Wong, M. W. Auger, S. Hilbert, V. Bonvin and S. Birrer, *et al.* Mon. Not. Roy. Astron. Soc. **490**, no.2, 1743-1773 (2019) [arXiv:1907.02533 [astro-ph.CO]].
- [73] S. Birrer, T. Treu, C. E. Rusu, V. Bonvin, C. D. Fassnacht, J. H. H. Chan, A. Agnello, A. J. Shajib, G. C. F. Chen and M. Auger, *et al.* Mon. Not. Roy. Astron. Soc. **484**, 4726 (2019) [arXiv:1809.01274 [astro-ph.CO]].
- [74] S. H. Suyu, T. Treu, S. Hilbert, A. Sonnenfeld, M. W. Auger, R. D. Blandford, T. Collett, F. Courbin, C. D. Fassnacht and L. V. E. Koopmans, *et al.* Astrophys. J. Lett. **788**, L35 (2014) [arXiv:1306.4732 [astro-ph.CO]].
- [75] C. E. Rusu, K. C. Wong, V. Bonvin, D. Sluse, S. H. Suyu, C. D. Fassnacht, J. H. H. Chan, S. Hilbert, M. W. Auger and A. Sonnenfeld, *et al.* [arXiv:1905.09338 [astro-ph.CO]].